High resolution DTI of Localized volume, using 3D singleshot STimulated EPI

E-K. Jeong[1], S-E. Kim[1], E. G. Kholmovski[1], D. L. Parker[1]

[1]Radiology, University of Utah, Salt Lake City, Utah, United States

INTRODUCTION Diffusion tensor MRI (DT-MRI), using conventional 2D singleshot diffusion weighted-EPI (2D ss-DWEPI), is limited to intracranial applications far from the sinus, due to the severe geometric distortion caused by strong non-linear local magnetic fields at or near tissue/air or tissue/bone interfaces. Although susceptibility induced distortions can be reduced by using multishot DW acquisition techniques, these multishot techniques, in general, suffer from artifacts caused by phase errors induced by small local or global motions during the large diffusion gradients. These artifacts cause inaccuracy in diffusion measurement. 3D singleshot interleaved multiple inner-volume stimulated echo planar imaging (3D ss-IMIV-DWSTEPI) is presented as a novel technique to perform 3D singleshot DW imaging (DWI) and DTI of a restricted 3D volume, which completes entire k-space acquisition after a single diffusion-preparation. This technique is advantageous for high-resolution 3D DTI, because it provides increased SNR and contiguous thin slices, and is immune to motion artifact.

METHODS 3D ss-IMIV-DWSTEPI acquires the entire 3D k-space data from a limited 3D volume in a singleshot after diffusion prepared (DP) driven-equilibrium (DPDE). DPDE contains 90° excitation, double-inversion for inner-volume imaging, 3 reference gradient echoes for EPI correction, diffusion-weighting, dephasing gradient, 90° tipup, and spoiling gradient. The imaging part combines stimulated echo imaging and echoplanar readout. The reduced FOV along the phase-encoding direction was implemented using an improved method for IMIV imaging with a pair of 180° RF pulses, which restored longitudinal magnetization of other slabs.[1] Eq. (1) describes the longitudinal magnetization just before the nth imaging RF pulse with respect to the previous longitudinal magnetization M^z_{n-1}.[2]:

$$M_n^z(\vec{r}) = M_o(\vec{r})\left(1 - e^{-\tau/T_1(\vec{r})}\right) + M_{n-1}^z(\vec{r}, t_{n-1}) \cdot \cos\alpha_{n-1} \cdot e^{-\tau/T_1(\vec{r})} \quad (1)$$

Here, α_n is the flip angle of the nth imaging RF pulse and τ is the duration of each segment. The two terms are the freshly recovered and DP magnetization, respectively. Signal from the first term, which is not diffusion weighted, is spoiled after each excitation by the rephasing crusher gradient, and the measured NMR signal reflects only DP magnetization which undergoes T_1 decay.

All imaging studies were performed on a 3 Tesla MRI scanner (Siemens Medical Solutions, Erlangen, Germany). Typical imaging parameters include the imaging matrix (192~256)x48x(8~32) with (1.25 mm)^3 isotropic spatial resolution, TE=75 ms, for diffusion weighting b = 750 s/mm^2, and 7 non-linear diffusion encodings. Stejskal-Tanner diffusion waveform with an added bipolar gradient pair was applied for diffusion preparation. 5/8 partial Fourier acquisition was used in both phase- and slice-encoding directions, to reduce actual data sampling duration. Center-out slice-ordering indicated at the bottom of Fig. 1b was applied to improve SNR. The flip angle was varied along the stimulated echotrain to reduce blurring in the slice-selective direction due to magnetization decay.

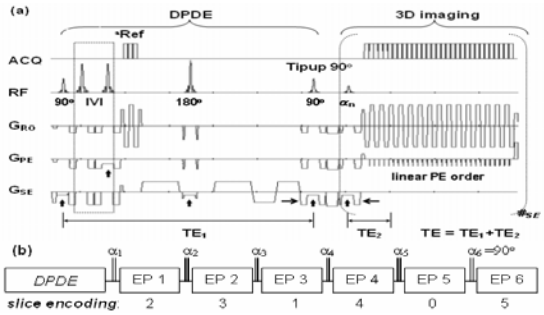

Fig. 1. *Pulse diagram of 3D ss-IVIM-DWSTEPI, consisting of DPDE and 3D data acquisition. A complete set of k_y views are acquired after each α RF pulse. Inner-volume imaging was used to define the reduced phase FOV. The imaging echotrain is repeated for all actual slice-encodings as shown in (b). The duration of each readout segment was about 40 ms. The horizontal arrows → and ← represent the dephasing- and rephasing-crusher gradients, respectively.*

RESULTS & DISCUSSIONS Plots (a, b) in Fig. 2 demonstrate (a) signal decay along the total stimulated echoes with phase-/slice-encoding gradients turned off, and (b) the resulting point-spreading function which indicates a 1.8 pixel-wide blurring in the slice-encoding direction. The images in Fig. 2c are several center slices of an agar phantom showing excellent resolution in the slice (left-right) direction. DTI of the midbrain of a healthy volunteer (Fig. 3) demonstrates the tensor MRI capability of 3D ss-IVIM STEPI for in-vivo application. The susceptibility artifact is minimal at/near the air/tissue and bone/tissue interfaces because the actual ETL was only 31 in the given study. In our preliminary application of 3D ss-IMIV-DWSTEPI, the spatial resolution was limited by SNR. The spatial resolution of (1.0 mm)^3 may be achieved by using a higher-quality RF coil or increasing the number of averages.

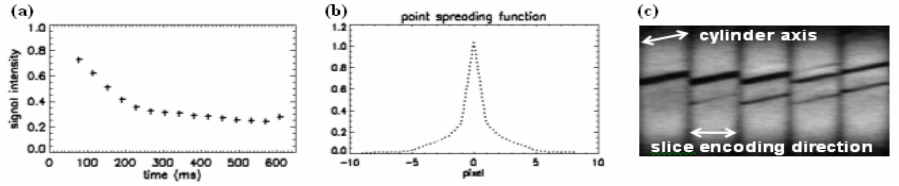

Fig. 2. (a) *Plot of the peak magnitude of the 15 stimulated echotrains and (b) the corresponding point-spreading function (PSF) for 3D ss-IMIV-DWSTEPI. (c) xz-plane images to show resolution in the slice direction. PSF width (FWHM) was 1.8 pixels. The resulting images shown in (c) are without any noticeable blurring in the slice direction.*

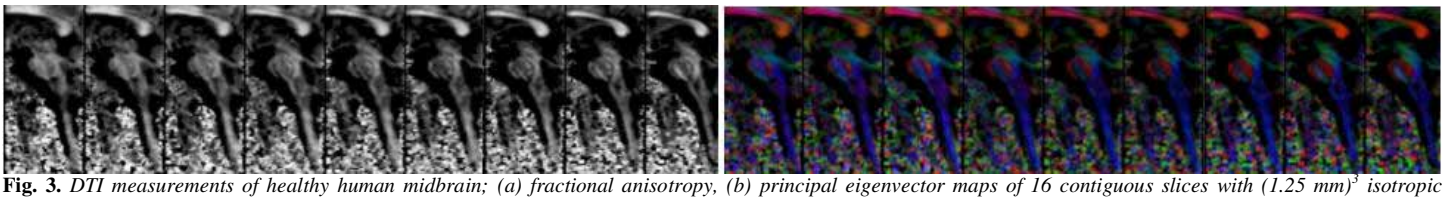

Fig. 3. *DTI measurements of healthy human midbrain; (a) fractional anisotropy, (b) principal eigenvector maps of 16 contiguous slices with (1.25 mm)^3 isotropic resolution. Corpus callosum demonstrates a high FA value and red color indicating left-right orientation. Cervical spinal cord is running head-foot direction (blue).*

CONCLUSIONS 3D ss-IMIV-STEPI can acquire the diffusion-weighted magnetization of a localized volume in a single excitation with high spatial resolution and very little susceptibility distortion. Even though its coverage is limited, localized 3D ss-IVIM STEPI may allow acquisition of high resolution DTI data from nearly any localized region of the body, overcoming the limitations of conventional 2D ss-DWEPI. This new technique not only reduces susceptibility artifacts, but also freezes most physiologic motion. In general, 3D ss-IMIV-STEPI should increases the accuracy of diffusion tensor measurements in high-resolution DTI of a localized volume.

ACKNOWLEDGEMENTS This work was supported by the Cumming Foundation, NIH grants R21 NS052424 and R01 HL57990, the Benning Foundation, and the Mark H. Huntsman Endowment.

REFERENCES

1. Jeong EK, Kim SE*et. al.* Magn Reson Med 2005;54. 2. Callaghan PT. Principle of Nuclear Magnetic Resonance Microscopy. Oxford: Oxford Science Publications; 1991. 3.Wheeler-Kingshott CA, Hickman SJ*et. al.* Neuroimage 2002;16:93-102.